Transfer and decay of an exciton coupled to vibrations in a dimer

Holger Schanz*
Institut für Physik, Humboldt-Universität, Invalidenstrasse 110, D-10115 Berlin, Germany

Ivan Barvík
Institute of Physics, Charles University, Ke Karlovu 5, 121 16 Prague, Czech Republic

Bernd Esser
Institut für Physik, Humboldt-Universität, Invalidenstrasse 110, D-10115 Berlin, Germany
(Received 13 June 1996; revised manuscript received 20 December 1996)

Transfer and decay dynamics of an exciton coupled to a polarization vibration in a dimer is investigated in a mixed quantum-classical picture with the exciton decay incorporated by a sink site. Using a separation of time scales, it is possible to explain analytically the most important characteristics of the model. If the vibronic subsystem is fast, these are the enhancement of nonlinear self-trapping due to the sink and the slowing down of the exciton decay for large coupling or sink strength. Numerical results obtained recently for the discrete self-trapping (DST) approximation to the model are quantitatively explained and dynamic effects beyond this approximation are found. If the vibronic subsystem is slow, the behavior of the system follows closely the predictions of the adiabatic approximation. In this regime, the exciton decay crucially depends on the initial conditions of the vibronic subsystem. In the transition regime between the adiabatic and DST approximation, complex dynamics is observed by numerical computation. We discuss the correspondence to the chaotic behavior of the excitonic-vibronic coupled dimer without trap. [S0163-1829(97)06317-0]

I. INTRODUCTION

The purpose of this paper is to study the interplay between a coherent transfer regime of an exciton and two processes leading to the loss of the linear character of the exciton transfer, namely trapping of the exciton at a sink site with a prescribed sink rate Γ and the coupling to intramolecular polarization vibrations. A lot of work has been done on exciton transfer theories during the last decades. Beginning with the microscopic treatment by Haken and Reineker[1] and Grover and Silbey[2] a number of theories such as the continuous time random walk (CTRW),[3] the Pauli master equation (PME),[4] the generalized master equation (GME),[5] the stochastic Liouville equation (SLE), and the Haken-Strobl-Reineker (HSR) model (see Ref. 6, and references therein) were developed and mainly directed to obtaining equations which describe the coupled coherent and incoherent motion of the excitation.

Trapping of quasiparticles due to a sink site constitutes an important phenomenon in many molecular systems. In photosynthesis, for instance, an exciton in a harvesting antenna transfers its energy to a reaction center, where it can be trapped. Electron transfer processes then follow. Pearlstein and Zuber were the first who recognized that the consequences of a sink on the energy transfer processes are different in the coherent and incoherent regimes (see Ref. 7 and references therein). Cápek and Szöcs[8] pointed out the necessity of a transformation of the memory functions in presence of a sink. They also gave a prescription for a proper inclusion of the sink into the HSR model. This found application, e.g., in computer simulations of the excitation transfer in photosynthetic systems.[9,10] Recently, a form of purely coherent memory functions was derived and shown to have important consequences for the excitation transfer.[11] Memory functions were also used to obtain characteristics entering the CTRW description including a sink.[12] An interesting feature of the exciton dynamics in the presence of a very strong sink is the inhibition of the transfer towards the sink site.[9,10,13] This leads to an *increasing* exciton life time with increasing sink rate.

The coupling between electronic and vibronic degrees of freedom in molecular and condensed media is another basic mechanism influencing transfer properties of electronic excitations in these systems. The investigation of its consequences started from the polaron problem in solid states (see, e.g., Ref. 14, and references therein; for exciton-phonon interaction see Ref. 15) and continued with the study of the influence of the vibronic bath variables on the excitation transfer properties in the framework of the generalized master equation[5] and stochastic Liouville equation approaches.[6]

With the development of the theory of dynamical systems it has become attractive to analyze the implications of electronic-vibronic couplings employing concepts and methods of this field. Using such a dynamic system approach we study the detailed picture of the time evolution of a small number of relevant variables of the system, which are assumed to interact weakly with the environment. Recent experimental developments in the field of ultrashort time-resolved spectroscopy (see, e.g., Ref. 16) seem to make a direct observation of this time evolution possible in the near future.

A remarkable feature of the simplest excitonic-vibronic coupled model—the dimer—is the possibility of self-trapping, i.e., unequal time averaged occupation probabilities on the two sites of the configuration. The easiest way to obtain this effect from a coupling to vibrational degrees of freedom

leads to the two-site discrete self-trapping (DST) equation[17–19] which is a nonlinear but self-contained equation of motion for the excitonic site occupation amplitudes. More sophisticated approaches take the dynamics of the vibrations explicitly into account by using a mixed quantum-classical description[20,21] or by treating the coupled system quantum mechanically.[22] The effect of dissipation on self-trapping was also studied by various authors.[23–25]

The investigation of the exciton transfer on relatively small molecular aggregates such as dimers or triades is of much interest for clarifying the applicability of exciton transfer theories to experimental situations such as described in Refs. 26 and 27. Moreover they may serve as a reasonable first approximation in order to understand, at least qualitatively, some processes in very complicated systems such as photosynthetic units with their antenna systems and reaction centers[28] which can hardly be treated as a whole. Consider for example the photosynthetic membrane of purple bacteria.[29] The reaction center is surrounded by ringlike core structures LH1 of bacteriochlorophylles. Peripheral ring subunits LH2 which are placed around and inbetween the LH1 structures, help to facilitate the energy transfer from the antenna to LH1 and then to the reaction center. Experimental investigation during the last years has shown[28] that the exciton transfer inside and also between the LH2 and LH1 rings takes place within a time of the order of some tens of femtoseconds and a few picoseconds, respectively. Hence the last step—the transfer of the exciton from the LH1 subunits to the reaction center, which takes a time of the order of some tens of picoseconds, is much slower and essentially determines the total time from the exciton creation until its destruction at the reaction center by a charge separation. It is generally accepted that the exciton comes probably by an incoherent hop at a contact place from LH2 to LH1 and then spreads very quickly over LH1 within a time of only several hundert femtoseconds. Therefore the interesting last step in the scenario can be modeled as transfer inside a dimer. The monomer where the exciton is initially created represents the whole ring LH1, and the other monomer is a sink site corresponding to the reaction center. In some bacteria the very large time needed for the energy transfer on this dimer has simple geometrical reasons such as a large distance from the LH1 ring to the reaction center. However, this does not seem to be a satisfactory explanation in all cases and therefore it is interesting to study other possible mechanisms leading to a very large exciton life time such as the above-mentioned self-trapping due to electronic-vibronic coupling and the slowing down of the transfer towards the sink for large trapping rates.

Although the influences of vibronic coupling and trapping on transport properties have been investigated separately in great detail, the combination of both, which can be important in the application of the transfer theory, has rarely been addressed in the past. In a recent paper[30] we have studied the interplay between vibrational coupling and trapping due to a sink site for a dimer and a trimer in the framework of the DST approximation. In the present paper we focus our interest on the exciton dynamics in a molecular dimer but explicitly include the coupling to vibrations using a mixed quantum-classical description,[20,21] which is justified whenever the quantum fluctuations in the vibronic subsystem are negligible. The model we use will be specified and developed further in Sec. II, where we also indicate the modifications leading to the DST equation.

Section III is devoted to the derivation of various self-contained equations for the total occupation probability based on some separation between the different time scales of the system. In particular, we will generalize the analysis of the fixed points for the excitonic-vibronic coupled dimer without sink[21] to the present system and in this way obtain an overall description of the phase space which allows us to understand qualitatively the dynamics for various initial conditions. We shall also point out in Sec. III A what is inherited in our more complex model from the DST approximation and which dynamic effects are beyond it. Since the mixed quantum-classical description we are using in this paper can be justified best for small oscillator frequencies, we pay much attention to this adiabatic regime, too. As we shall see, the assumption of slow vibrations is just the antipode of the DST case and therefore a qualitatively new behavior can be expected from it (Sec. III B).

Using the results of Sec. III as well as numerical computations we will discuss the time dependence of the total occupation probability and the relative site occupation probabilities for some solutions with specified initial conditions in Sec. IV. A summary of our results can be found in Sec. V.

II. DESCRIPTION OF THE MODEL

A. The Hamiltonian

We consider the dynamics of an exciton moving on a molecular dimer. At each of the two monomers the exciton is allowed to interact with an intramolecular vibronic degree of freedom. Thus, the Hamiltonian of our model contains excitonic, vibronic, and interaction parts denoted by H_{exc}, H_{vib}, and H_{int}, respectively

$$H = H_{\mathrm{exc}} + H_{\mathrm{vib}} + H_{\mathrm{int}}. \tag{1}$$

H_{exc} describes a two site model

$$H_{\mathrm{exc}} = \sum_n \epsilon_n c_n^* c_n + \sum_{n \neq m} V_{nm} c_n^* c_m \tag{2}$$

with $n,m = 1,2$. c_n is the probability amplitude of the exciton to occupy the nth molecule and V_{nm} the transfer matrix element due to dipole-dipole interaction. In a standard two site model, the ϵ_n are real quantities and correspond to the local site energies of the exciton. Here, we allow ϵ_2 to contain a negative imaginary part in order to describe the decay of the exciton on the sink site 2. Since we are not interested in the effect of a site energy difference on the exciton dynamics in the present context, we set

$$\epsilon_1 = 0, \quad \epsilon_2 = -i\frac{\Gamma}{2}, \tag{3}$$

which is equivalent to the extended sink model for the exciton decay introduced in Ref. 8 on the density matrix level. This model has been shown to solve the problem of a consistent description of exciton trapping at a sink meeting basic physical requirements such as positive occupation probabilities.

The vibrational part H_{vib} is taken as the sum of the energies corresponding to intramolecular vibrations at each of the monomers for which we use the harmonic approximation

$$H_{\mathrm{vib}}=\sum_n \frac{1}{2}(p_n^2+\omega_n^2 q_n^2). \tag{4}$$

q_n, p_n, and ω_n are the coordinate, the canonic conjugate momentum and the frequency of the intramolecular vibration of the nth molecule, respectively.

The interaction Hamiltonian takes into account that the exciton energy depends on the molecular configuration of the monomers which is expressed by the coordinates q_n. Using a first-order expansion in q_n one has

$$H_{\mathrm{int}}=\sum_n \gamma_n q_n c_n^* c_n, \tag{5}$$

where γ_n are some coupling constants. In order to restrict the number of free parameters as much as possible we will assume that the dimer is symmetric except for the additional sink term on site 2, i.e., $\omega_1=\omega_2=\omega$, $\gamma_1=\gamma_2=\gamma$, and $V_{12}=V_{21}=-V$.

In what follows we will use a mixed quantum-classical description of the dynamics, i.e., we treat the vibronic degrees of freedom in the classical approximation while retaining the quantum wave function for the excitonic two site system. The approximation can be justified over a finite interval in time which increases as the oscillator frequencies and coupling constants decrease. When this time range exceeds the lifetime of the exciton the mixed quantum-classical picture describes correctly the decay of the excitation.

Using units with $\hbar=1$ we obtain from Eqs. (1)–(5) the equations of motion

$$id/dtc_1=\gamma q_1 c_1-Vc_2, \tag{6}$$

$$id/dtc_2=\left(-i\frac{\Gamma}{2}+\gamma q_2\right)c_2-Vc_1, \tag{7}$$

$$d/dtq_n=p_n, \tag{8}$$

$$d/dtp_n=-\omega^2 q_n-\gamma|c_n|^2. \tag{9}$$

We believe that the excitonic-vibronic coupled dimer as introduced in this section is a very basic model and represents a topic of interest in its own right. We will therefore not restrict the discussion by fixing the parameter values using the particular realization which we described in the Introduction. In fact the available experimental data also do not allow us to do so with sufficient accuracy which is due to the complicated structure of the photosynthetic units and the rather crude approximation by a simple dimer. Instead we will try to discuss the properties of our model covering the largest possible range of values for the relevant parameters, which will be specified in the next subsection.

B. Reduced equations of motion

For a numerical investigation Eqs. (6)–(9) are well suited and we have integrated them in order to obtain the results that will be presented in Sec. IV. The analytical treatment of Sec. III, however, requires us to reduce the number of variables and free parameters as much as possible. Therefore we will now rewrite the equations of motion (6)–(9) using appropriate dimensionless variables and parameters.

The excitonic subsystem can be described by a point on the Bloch sphere which is usually given in Cartesian coordinates. Here we prefer to parametrize the Bloch sphere in spherical coordinates R, θ, and ϕ. They can be defined in terms of the density matrix of the two-site system $\rho_{mn}=c_m c_n^*$ $(n,m=1,2)$

$$\begin{aligned} R&=\rho_{11}+\rho_{22},\\ R\cos\theta&=\rho_{22}-\rho_{11}\quad(0\leqslant\theta\leqslant\pi),\\ e^{i\phi}R\sin\theta&=2\rho_{12}\quad(-\pi<\phi\leqslant\pi). \end{aligned} \tag{10}$$

Due to the trapping of the exciton the radius of the Bloch sphere $R(t)$ which is the total probability to find an exciton on either of the two sites is not constant but a monotonically decreasing function of time with $R(0)=1$.

Besides the total occupation probability R the difference of the occupation of the two sites is of interest. It is determined by the angle θ since we have

$$|c_1|^2=\frac{1-\cos\theta}{2}R,\quad |c_2|^2=\frac{1+\cos\theta}{2}R. \tag{11}$$

The phase ϕ has no direct physical interpretation. We note that ϕ is not well defined at the points $\theta=0$ and $\theta=\pi$. This can be circumvented by directly considering the time dependence of the density matrix at these points and will not affect the following.

When deriving the equations of motion for the new variables from (6)–(9) one observes that only the difference q_2-q_1 couples to the excitonic degrees of freedom. Therefore we can introduce a dimensionless difference coordinate and the conjugate momentum

$$Q=\sqrt{V}(q_2-q_1),\quad P=\frac{1}{2\sqrt{V}}(p_2-p_1) \tag{12}$$

and reduce the number of independent variables in this way by two. The reduced equations of motion for the remaining five variables are obtained after the introduction of a dimensionless time

$$\tau=2Vt \tag{13}$$

and dimensionless parameters

$$p=\frac{\gamma^2}{2V\omega^2},\quad r=\frac{\omega}{2V},\quad g=\frac{\Gamma}{4V} \tag{14}$$

describing the strength of the electronic-vibronic coupling, the frequency ratio of the two interacting subsystems and the strength of the sink, respectively. We find

$$\dot{R}=-g(\cos\theta+1)R, \tag{15}$$

$$\dot{\theta}=g\sin\theta+\sin\phi, \tag{16}$$

$$\dot{\phi}=\cot\theta\cos\phi+\sqrt{2p}rQ, \tag{17}$$

$$\dot{Q}=P, \tag{18}$$

$$\dot{P}=-r^2Q-\sqrt{p/2}rR\cos\theta. \tag{19}$$

In these equations $(\cdot)$ denotes $d/d\tau$.

C. The DST approximation

One standard way to simplify the dynamics of excitonic-vibronic coupled systems is to assume that the vibronic degrees of freedom instantaneously adapt to the state of the excitonic subsystem and always remain in the ground state prescribed by it. Applied to Eqs. (6)–(9), this assumption results in the DST equations mentioned in the introduction.

Within our effective dynamic model (15)–(19) the DST approximation can be justified assuming a separation of time scales. The time scale for the (free) transfer of the excitation between the two sites of the dimer has been normalized to 1 when the equations of motion were written using the dimensionless time τ Eq. (13). Another relevant characteristic time of our system is the period of the oscillator which is $\sim 1/r$. Now we assume that the vibronic degrees of freedom are much faster than the exciton, i.e., $r \gg 1$. In this case the oscillator coordinate completes many cycles during a time of the order 1 which is relevant for the slow excitonic subsystem. Consequently, dynamic self-averaging over the fast oscillator coordinate occurs and Q in Eq. (17) can be replaced by its time average. For the harmonic oscillator (Q,P) this average is given for arbitrary amplitude by the oscillator ground state which is determined by the state of the excitonic subsystem and which represents at the same time the only fixed point of the oscillator dynamics, i.e., formally we can introduce the DST approximation by requiring quasistationarity in the vibronic variables $\dot{Q}=\dot{P}=0$. After substitution of the time average

$$Q_{\mathrm{DST}}=-\frac{1}{r}\sqrt{\frac{p}{2}}R\cos\theta \tag{20}$$

for Q, Eq. (17) is replaced by

$$\dot{\phi}=\cot\theta\,\cos\phi-pR\cos\theta. \tag{21}$$

Together with Eqs. (15) and (16) this equation governs the DST dynamics of the model.

An analytical justification for the averaging procedures applied in this and the following sections can be given using mathematical tools that were developed in the theory of nonlinear differential equations (see, e.g., Ref. 32) and will not be discussed here. Instead we confirm the resulting equation (21) by the numerical simulations for $r \gg 1$ presented at the end of this paper.

The derivation of the DST approximation using fast oscillator dynamics is questionable although it seems straightforward within the mixed quantum-classical description to which this paper is confined. However, the assumption $r \gg 1$ means that the mixed quantum-classical description itself loses its justification and should be replaced by a full quantum treatment. More consistent ways to obtain the DST limit are based on dissipation due to a quantum heat bath[24] and therefore beyond the scope of our model.

The DST equation is known to reproduce at least qualitatively some remarkable features which the full dynamic system[21] displays for an arbitrary value of r, e.g., the bifurcation in the phase space for $p=1$,[17] the resulting possibility of self-trapped solutions for coupling strengths above this value,[18] and the possibility of dynamical chaos when an external perturbation is applied.[19] We can therefore consider the results obtained in Ref. 30 within the DST approximation for a dimer with sink as a guiding line for the effects that can be expected in the present more complete treatment.

III. QUASISTATIONARY DECAY MODES

A. Fixed points for quasistationary total occupation

Beside the free exciton transfer time and the oscillator period there is a third relevant time scale which controls the decay of the excitation but is not necessarily given by the inverse sink rate $1/g$ as we shall see. It is the aim of the present section to derive quasistationary solutions of the equations of motion (15)–(19) and the corresponding self-contained equation for the decay of the total occupation probability $R(\tau)$ under the assumption that that the exciton decay is much slower than the oscillator dynamics. The opposite case of an oscillator which is slower than the excitation decay will be treated in the next subsection.

In the following we discuss the fixed points of Eqs. (16)–(19) with $R(\tau)$ treated as a slowly varying parameter. According to Eq. (15), this is justified when either the sink rate g is very small or the quasistationary state has a site occupation difference which is strongly biased towards the site without sink $\cos\theta \sim -1$. The exact condition for the applicability of our approach will be given below. The equations (18) and (19) yield for a fixed point $P=0$ and $Q=Q_{\mathrm{DST}}$, i.e., the location of the fixed points is the same for the system with the full oscillator dynamics included and for the DST equations. Equations (16) and (17) allow for two different pairs of fixed points on the Bloch sphere classified in what follows as detrapped and self-trapped states. The stability exponents for any of these points can be obtained from a linearization of the equations of motion (16)–(19) around the fixed point which yields the characteristic equation

$$0=(\lambda^2+r^2)\left([\lambda+\sin\phi\,\cot\theta][\lambda-g\cos\theta]+\frac{\cos^2\phi}{\sin^2\theta}\right) -r^2pR\cos\phi\,\sin\theta. \tag{22}$$

1. Detrapped states

For sufficiently small sink rate $g \leqslant 1$ we obtain two fixed points at

$$\sin\phi=-g, \quad \cos\phi=\pm\sqrt{1-g^2}, \tag{23}$$

$$\cos\theta=0. \tag{24}$$

Because of Eq. (24) the occupation probabilities for the two sites are the same and we call the fixed points $A^{\pm}$ detrapped states. The point A^{+} at $\cos\phi>0$ can be considered as a generalization of the bonding state in the system without sink

whereas the point A^- at $\cos\phi<0$ corresponds to the antibonding state. The stability exponents of these fixed points are given by

$$\lambda^2=-\frac{r^2+\cos^2\phi}{2}\pm\sqrt{\left(\frac{r^2-\cos^2\phi}{2}\right)^2+r^2pR\cos\phi}. \tag{25}$$

For A^+ the argument of the square root is always positive and the pair of stability exponents corresponding to the negative sign in Eq. (25) is purely imaginary. The other pair consists of two imaginary or two real exponents with opposite signs such that the fixed point A^+ is stable elliptic if $(pR)^2+g^2<1$ and unstable hyperbolic otherwise.

For A^- the stability is determined by the argument of the square root in Eq. (25). If it is positive, the point is a stable elliptic center and this is always the case in the adiabatic regime $r\to 0$, in the opposite DST case $r\to\infty$ or for arbitrary parameters at large times since then $R\to 0$. Only for sufficiently large p the argument of the square root may temporarily be negative. The stability exponents then acquire real parts with opposite signs and the point A^- renders unstable hyperbolic.

For the DST case $r\gg 1$ one pair of stability exponents which is given by $\lambda=\pm ir$ corresponds to the fast oscillations around the DST solution whereas the other pair of exponents

$$\lambda^2=\cos\phi(pR-\cos\phi) \tag{26}$$

describes the stability of the DST solution itself.

We note, that the positions of the two fixed points $A^\pm$ do not depend on R and are thus constant in time. For the full system with R time dependent they represent, therefore, special time-dependent states in which the distribution of the excitation over the two sites is constant, just the total occupation decreases exponentially at a rate g

$$\dot R=-gR. \tag{27}$$

When these fixed points are stable, a state prepared in their vicinity will remain there and decay at a mean rate g with some oscillations superimposed.

2. Self-trapped states

For $(pR)^2+g^2\geqslant 1$ there exist two other fixed points $B^\pm$ with biased site occupation probabilities, i.e., self-trapped states:

$$\sin\theta=\frac{1}{\sqrt{(pR)^2+g^2}},\quad \cos\theta=\pm\sqrt{1-\sin^2\theta}, \tag{28}$$

$$\sin\phi=-g\sin\theta,\quad \cos\phi=pR\sin\theta. \tag{29}$$

The existence of these two fixed points corresponds exactly to the range of parameters for which the fixed point A^+ is hyperbolic and for $(pR)^2+g^2=1$ the points A^+ and $B^\pm$ merge into a single one. So we have established a generalization of the pitchfork bifurcation of the system without sink.[21] The difference is that the bifurcation parameter no longer depends exclusively on the coupling strength p. Rather it contains along with p the strength of the sink g and the total occupation probability R which is a function of time. If $g<1$ the fixed points $B^\pm$ will disappear for large times when $R\to 0$ and we can speak of a dynamic bifurcation. On the other hand, when $g>1$ the detrapped states A do not exist anymore and there is no bifurcation in the course of time.

Without sink the fixed points $B^\pm$ are stable elliptic centers and in their vicinity there exist solutions which remain self-trapped for all times. In the present case the stability exponents have to be determined from the quartic equation

$$0=(r^2+\lambda^2)([\lambda-g\cos\theta]^2+p^2R^2)-(rpR\sin\theta)^2, \tag{30}$$

which does not allow for an easy solution. We shall see below, that the fixed points $B^\pm$ due to their time dependence do not represent quasistationary solutions unless the bifurcation parameter $\sin^{-2}\theta=(pR)^2+g^2$ is far enough above the bifurcation value 1. Therefore we simplify Eq. (30) under the assumption $\sin^2\theta\ll 1$ and drop the second term. Then, there are two pairs of solutions for the stability exponents. One of them is purely imaginary $\lambda=\pm ir$ and the other one contains a real part as well:

$$\lambda=g\cos\theta\pm ipR. \tag{31}$$

Again, for $r\to\infty$ the first pair describes the oscillations around the DST solution and the other one the stability of the DST solution which can alternatively be obtained from a linearization of Eqs. (16) and (21) without further approximations as

$$\lambda=g\cos\theta\pm i|\cos\theta|pR. \tag{32}$$

Note that $\pm$ in Eq. (28) stands for the two different fixed points, whereas the $\pm$ in Eqs. (31) and (32) corresponds to two different stability exponents λ of the same fixed point.

The character of the fixed points $B^\pm$ is determined by the real part of λ. For B^+ with an occupation bias towards the sink site $(\cos\theta>0)$ we have a repeller, whereas the point B^- with a low occupation probability at the sink site $(\cos\theta<0)$ is a stable attractor.

It is less clear than for the detrapped states that the fixed points $B^\pm$ which were obtained under the assumption of a constant total occupation have some interpretation for the full system since their location does depend on $R(\tau)$. However, we will show now that at least B^- can represent an attractor and a quasistationary solution for the complete equations of motion (15)–(19) when we are sufficiently far away from its threshold of existence, i.e., when the bifurcation parameter is sufficiently large

$$\sin^2\theta=\frac{1}{g^2+(pR)^2}\ll 1. \tag{33}$$

For this purpose we have to show that the change in the position of B^- is much slower than the relaxation towards this fixed point. The latter occurs on a time scale given by Eq. (31) as $1/g$, while the oscillations around the fixed point have a period $2\pi/r$ and will be averaged out provided this time is small enough.

The velocity of the fixed point location can be estimated after inserting Eq. (15) into Eqs. (28) and (29). We obtain

$$|\dot{\theta}| = g(pR)^2 \frac{\sin^3\theta(1+\cos\theta)}{|\cos\theta|}$$
$$\sim \frac{g(pR)^2}{2}\sin^5\theta$$
$$< \frac{g}{2}\sin^3\theta,$$

$$|\dot{\phi}| = (gpR)^2 \frac{\sin^3\theta(1+\cos\theta)}{\cos\phi}$$
$$\sim \frac{g^2 pR}{2}\sin^4\theta$$
$$< \frac{g}{2}\sin^2\theta$$

and conclude that the position of B^- always changes slowly when $\sin^2\theta \ll 1$ and in particular the relaxation towards the attractor is much faster. If, moreover, $g/2\ \sin^2\theta \ll r$ the oscillations around the fixed point average out in Eq. (15) and we can consider $\{R(\tau),\ \theta[R(\tau)],\ \phi[R(\tau)]\}$ as an attractor for the full system. This condition is automatically satisfied when $r > 1$ (e.g., in the DST regime), but in the adiabatic regime $r \ll 1$ the assumption of quasistationarity of B^- may not be valid or restricted to a short interval in time. This case is considered in the next subsection. Once the system is close to the attractor B^- the excitation decay is approximately governed by the equation

$$\dot{R} = -\frac{g/2}{(pR)^2 + g^2} R. \tag{34}$$

If, moreover, the sink rate is dominant $pR < g$ we obtain from Eq. (34) the interesting effect that the decay rate *decreases* for increasing sink rate g. The reason is that the location of B^- is strongly shifted to the site without sink such that the probability to find the exciton on the sink site becomes very small. This behavior has previously been studied without coupling to vibrations.[9] When we have $pR/g \to 0$, which is always the case for $\tau \to \infty$, Eq. (34) implies an exponential decay of the exciton with the rate $1/2g$. From Eqs. (27) and (34) we conclude that the fastest quasistationary decay of the excitation is realized for small electronic-vibronic coupling and a sink rate $g = 1$.

Self-trapping on the site with sink is not immediately destroyed when the sink becomes effective. Though the state B^+ is a repeller, the solution can oscillate with slowly increasing amplitude around this fixed point provided that g is not too large. In this case B^+ can control the dynamics for some finite time which then leads to an *enhanced* excitation decay.

B. The adiabatic regime

In the previous subsection we considered quasistationary dynamics of the excitation under the assumption that the decay of the exciton represents the slowest process in the system. This assumption breaks down when the system is in the adiabatic regime $r \ll 1$. Then the decay is an essentially nonstationary process leading to the disappearance of the exciton before the oscillator has gone through a large number of cycles.

Opposite to the derivation of the DST equation we can now assume that the exciton completes many oscillations on the time scale of the oscillator. Again we want to exploit this fact by averaging over the variables of the fast subsystem and replacing them by their mean value, but in contrast to the harmonic oscillator of the DST case, the equations of motion for the excitonic variables have two fixed points for a given Q which are obtained by setting the left-hand side of Eqs. (17) and (16) to zero. This results in

$$\sin\phi = -g\sin\theta, \quad \cos\phi = -\sqrt{2pr}\,Q\tan\theta \tag{35}$$

and combining these two equations we find

$$g^2\sin^2\theta + 2pr^2Q^2\tan^2\theta = 1. \tag{36}$$

The latter equation determines the location of the fixed points which depends parametrically on Q. The stability exponents can be given in the form

$$\lambda = g\cos\theta \pm i\sqrt{2pr}\,|Q/\cos\theta|. \tag{37}$$

Equation (36) is a biquadratic equation in $\cos\theta$, i.e., the two fixed points have opposite signs for $\cos\theta$. Due to Eq. (37) this means that one of them is a stable attractor, the other one a repeller. Instead of writing down the explicit solution of Eq. (36), which is quite a lengthy expression though easily found, we would like to mention two limiting cases.

First we note, that as $g \to 0$ the two fixed points approach the well known lower and upper adiabatic states of the system without trap

$$\cos\theta = \pm\frac{\sqrt{2pr}\,Q}{\sqrt{1+2pr^2Q^2}}, \quad \cos\phi = \mp 1 \tag{38}$$

(see, e.g., Ref. 22 for the adiabatic potentials). The second important limiting case corresponds to a strong localization of the exciton on one of the two dimer sites ($\cos\theta \to \pm 1$). Assuming $g^2 + 2p\ r^2\ Q^2 \gg 1$ the solution approaches

$$\sin\theta = \frac{1}{\sqrt{g^2+2pr^2Q^2}}. \tag{39}$$

In particular, for a very large sink rate g the dependence on Q disappears and we have

$$\sin\theta = \frac{1}{g} \ll 1, \quad \sin\phi = -1. \tag{40}$$

In order to be able to replace the time average for the excitonic variables by the discussed fixed points we have to assume that the time scale given by Eq. (37) for the relaxation is sufficiently short, or that the oscillations around the fixed point do average out. Due to the nonlinear equations for the excitonic variables and in contrast to the derivation of the DST equation we have, in this latter case, to assume that the amplitude of the oscillations is small, i.e., the system has to be prepared close to one of the adiabatic states. If so, even the adiabatic state with $\cos\theta < 0$, which is in fact a repeller, can be considered quasistationary for some limited time.

A self-contained equation for the decay of the total excitation probability $R(\tau)$ can be derived under the assumption that the exciton is located close to the attractive quasistationary state. Then $\cos\theta$ may be replaced by the value prescribed by the oscillator coordinate Q according to Eq. (36) and is constant provided the oscillator dynamics is sufficiently slow to be completely disregarded during the lifetime of the exciton or if the position of the fixed point according to Eq. (40) does not depend on time due to a strong trap. Either case leads to an exponential decay of the excitation.

IV. THE TIME EVOLUTION OF THE SYSTEM

A. Parameter regions and initial conditions

In this section we turn to the investigation of the time evolution of particular solutions starting from explicitly specified initial conditions. According to the experimental situation in photosynthetic units described in the Introduction, where the exciton is always created at the site without sink, we set initially

$$c_1(0)=1, \quad c_2(0)=0. \tag{41}$$

This localized initial condition can also be realized in completely different experimental settings, e.g., when an exciton in a dimer is created using a femtosecond laser pulse with the appropriate duration and polarization.[31] Moreover, we would like to mention that the results of the previous section can be applied in the most straightforward way for the special case (41). The evolution for different initial conditions and the associated optical emission due to the spontaneous decay of excitons described by the sinkless DST dimer was investigated, e.g., in Ref. 33, where in particular the influence of chaotic dynamics occurring in the stochastic layer due to a perturbation of the DST solution was considered.

The initial conditions for the vibronic degrees of freedom which we have chosen are meant to take into account different physical possibilities to prepare the excitation and to provide enough variety to estimate the degree to which the excitonic variables depend on the details of the oscillator initial state. The resulting solutions will be referred to in the following way.

(1) *Bare exciton*: The first initial state we consider corresponds to a sudden creation of the exciton on the sinkless molecule when the vibrations are initially in an unrelaxed state $q_i(0)=0$, i.e., displaced from their ground states, and $p_i(0)=0$. The total energy for this initial condition is 0.

(2) *Polaron*: The second possibility is to assume a slow excitation such that initially the vibrational degrees of freedom are already relaxed to their new ground state with exciton. This is the initial condition which would be implied by the DST approximation: $q_1(0)=-\gamma/\omega^2$, $q_2(0)=0$, $p_i(0)=0$. The total energy of the polaron is $-\gamma^2/2\omega^2$, i.e., lower than the energy of the bare exciton.

(3) *Polaron with additional vibrational energy* [*Polaron* $(-)$ *and Polaron* $(+)$]: The different initial energies make a direct comparison between the bare exciton and the polaron difficult. Therefore we have taken into account a third possibility for the initial condition. Again we choose the configuration coordinate of the vibrations in the minimum of the potential after the exciton has been created. We supply, however, an initial momentum such that the total energy is 0 as for the bare exciton case. For this momentum we have two different possible directions, i.e., the polaron $(\pm)$ is specified by $q_1(0)=-\gamma/\omega^2$, $q_2=0$, $p_1(0)=\pm\gamma/\omega$, $p_2(0)=0$.

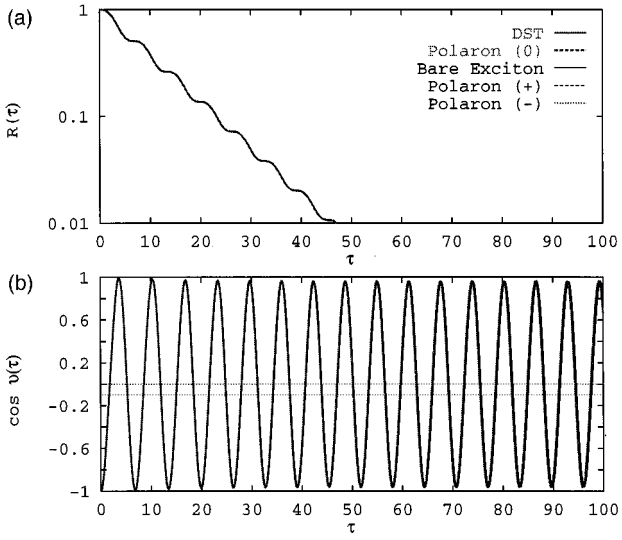

FIG. 1. Time dependence of the total occupation (a) and of the relative site occupation difference (b) for $g=0.1$, $p=1$, and $r=10$. Different oscillator initial conditions for the full dynamic model and the DST dynamics can hardly be distinguished for this parameter set. They are shown in this and all the following figures with the line types indicated in the upper part. In the bottom plot, $\cos\theta=1$ corresponds to the sink site and $\cos\theta=-1$ to the sinkless site where the exciton is created. The lower/upper horizontal line shows the location of the fixed point B^- at the time of the creation of the exciton $(R=1)$ and after its complete decay $(R=0)$, respectively.

We have performed a numerical integration of the coupled system of Eqs. (6)–(9) for the different described initial conditions. We display results for the total occupation probability $R(\tau)$ and the relative site occupation difference expressed by $\cos\theta(\tau)$ for various values of the oscillator frequency ranging from the high-frequency (DST) limit in Figs. 1–3 to the deeply adiabatic region in Fig. 8. We restrict the sink rate and the vibrational coupling to three representative cases: (i) weak sink $g=0.1$/weak coupling $p=1$ (Fig. 1); (ii) weak sink $g=0.1$/strong coupling $p=3$ (Figs. 2, 4, 6, and 8); (iii) strong sink $g=3$/strong coupling $p=3$ (Figs. 3, 5, and 7). For each set of parameters the results for the different initial conditions will be displayed in the same graph. They can be distinguished by the different line shapes annotated, e.g., in Fig. 1(a).

B. Time evolution in the DST approximation

Using the results of Sec. III A we can obtain a quite satisfactory description of the time evolution in the DST approximation that agrees with our numerical findings reported in Ref. 30. We have to distinguish three different cases with respect to the parameters p and g

(i) *Nearly linear regime* $g^2+p^2<1$. In this case throughout the whole time evolution the only fixed points present are the stable elliptic centers $A^{\pm}$ from Sec. III.A. The relative site occupation difference $\cos\theta$ will therefore oscillate with a

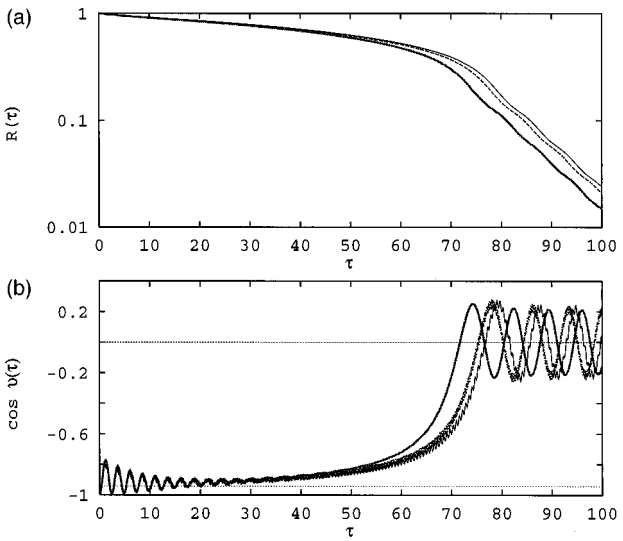

FIG. 2. Time dependence of the total occupation (a) and of the relative site occupation difference (b) for $g=0.1$, $p=3$, and $r=10$.

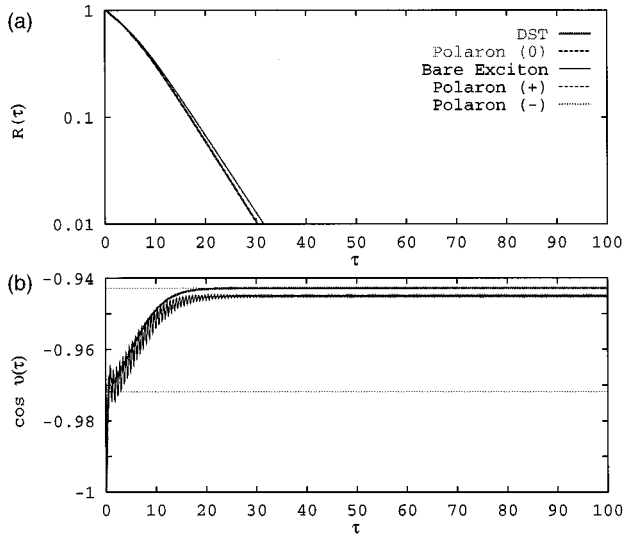

FIG. 3. Time dependence of the total occupation (a) and of the relative site occupation difference [(b)—DST, bare exciton, and polaron (0) only] for $g=3$, $p=3$, and $r=10$.

mean value $\cos\theta=0$. The decay of the total occupation probability is then approximately given by [Eq. (27)]

$$R(\tau)\sim e^{-g\tau}, \tag{42}$$

and is therefore very much like the case of the linear dimer.

An illustration for the described behavior is provided by Fig. 1, which is with $p=1$ and $g=0.1$ at the fringe of region (i). Since the transition between the parameter regions is smooth, we find in Fig. 1(a) a straight line indicating an exponential decay with some oscillations superimposed. The mean decay rate obtained from the figure is in good correspondence to Eq. (42) very close to 0.1 and the period of the oscillations in Fig. 1(b) is very close to 2π. This is the value for the free transfer of the excitation and corresponds to the asymptotic value for the stability exponent of the points $A^{\pm}$. However, the solution is actually not in the vicinity of one of these points. Rather it oscillates with a large amplitude and can therefore not be expected to be correctly described by a linearization around a fixed point. For instance, the time dependence of the stability exponent (26) is not reflected in the solution.

(ii) *Weak sink* $g<1$ *and strong coupling* $g^2+p^2>1$. In this case there exists the attractive fixed point B^- from Sec. III A when the system starts its evolution at $R(\tau=0)=1$. As a numerical example consider the DST curve of Fig. 2 which is the thick gray line. The system approaches the attractor after a time $\tau\sim 1/g$ and then decays on it according to Eq. (34). This is in general a nonexponential decay which is very much different from Eq. (42). If we assume strong nonlinearity $p\gg 1$, Eq. (34) can be approximated and results in

$$R(\tau)=\sqrt{1-\frac{g}{p^2}\tau}. \tag{43}$$

There will be oscillations around this mean behavior with an amplitude decreasing as the attractor is approached. The frequency Ω of these oscillations is given by the imaginary part of the stability exponent in Eq. (30) and decreases approximately as $\Omega\sim pR$ for strong nonlinearity. Indeed, the oscillations around the mean in Fig. 2(b) have a period which can be seen to increase starting from $T\sim 2.4$ which is close to the value 2.2 obtained from the imaginary part of Eq. (30). Then the oscillations die out at $\tau\sim 30$ thus confirming the attractive character of the fixed point B^-.

When the total occupation has decreased such that $g^2+(pR)^2\sim 1$, the attractor B^- does not exist anymore and the system will start oscillating with equal mean site occupation probabilities around one of the fixed points $A^{\pm}$ as in (i). The time τ_0 for the crossover from the algebraic decay (43) to an exponential behavior with decay rate g is approximately given by

$$\tau_0=\frac{p^2-1}{g}. \tag{44}$$

(iii) *Strong sink* $g>1$. Here the attractor B^- does exist throughout the evolution of the system. If the nonlinearity is very large there might be initially a nonexponential behavior as in (ii), but this will turn into an exponential decay as soon as the total occupation has decreased sufficiently for $g\gg pR$. Under the assumption $p\gg g$ which is, however, not satisfied in the numerical example Fig. 3, the approximate crossover time is obtained from Eq. (43) as

$$\tau_0=\frac{p^2-g}{g}. \tag{45}$$

In the asymptotic regime one has from Eq. (34)

$$R(\tau)\sim\exp(-[g-\sqrt{g^2-1}]\tau). \tag{46}$$

The DST solution represented by the thick gray line in Fig. 3 relaxes after a very short time to the attractor B^- whose initial and final position is marked by dotted horizontal lines. Due to the larger g compared to Fig. 2 the initial oscillations

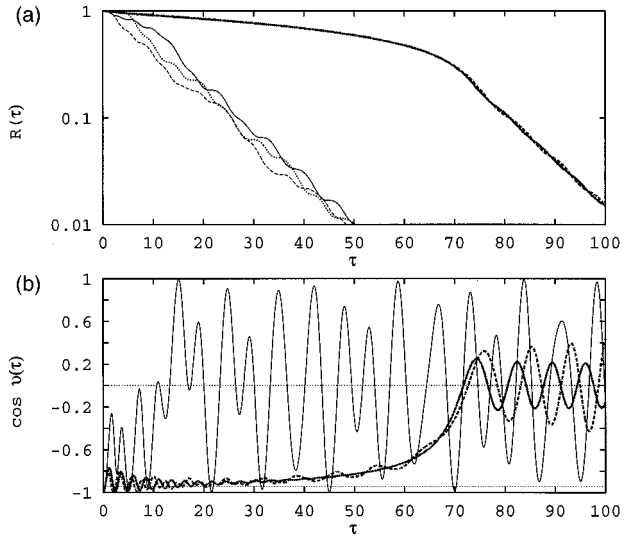

FIG. 4. Time dependence of the total occupation (a) and of the relative site occupation difference [(b)—DST, bare exciton, and polaron (0) only] for $g=0.1$, $p=3$, and $r=1$.

around B^- can hardly be observed. The crossover to constant relative site occupation probabilities and exponential decay occurs at $\tau\sim 20$.

C. Deviations from the DST approximation at large but finite oscillator frequency

The three different scenarios for the time evolution in the DST approximation which were described in the previous section remain valid for the full system with the oscillator frequency not too low, since the fixed points of Sec. III A still represent quasistationary decay modes. Using the numerical results displayed in Fig. 1–5 we will demonstrate this, discussing at the same time deviations from the DST solutions.

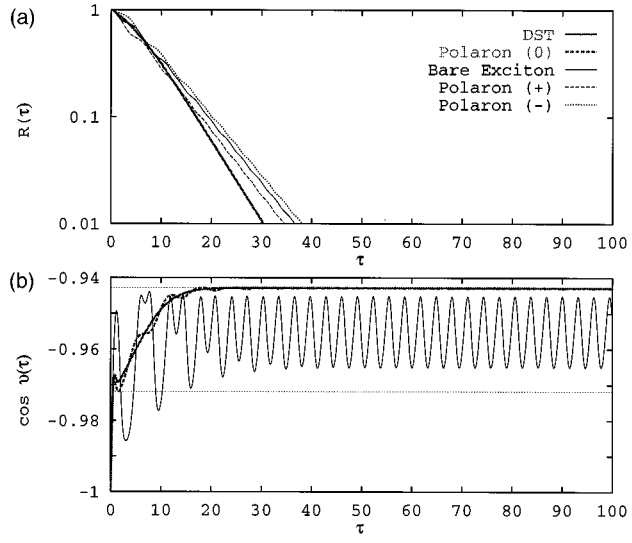

FIG. 5. Time dependence of the total occupation (a) and of the relative site occupation difference [(b)—DST, bare exciton, and polaron (0) only] for $g=3$, $p=3$, and $r=1$.

The degree of deviations from the DST solution will depend on the value of the parameter r and on the initial conditions for the oscillator. In particular for intermediate oscillator frequency it can be expected that the DST approximation describes the actual solution better the closer to it the initial condition for the oscillator is chosen. Indeed, the polaron (0) (dashed thick gray line), which is prepared in a DST state, cannot be distinguished at all from the DST curve in the plots for high oscillator frequency $r=10$ (Figs. 1–3) and follows it very closely in the plots for the intermediate frequency $r=1$ (Fig. 5). For small nonlinearity $p=1$ (Fig. 1) the same holds true for the other three solutions which are prepared with higher energy than the DST solution and in this case the initial conditions have no crucial influence on the dynamics down to the intermediate oscillator frequency $r=1$ (not displayed).

A systematic, though small deviation from the DST solution can be observed for stronger nonlinearity in the Figs. 2, 3, and 5. Here, a self-trapped state is approached by the polaron $(\pm)$ and the bare exciton solution as described for the DST case, but besides the familiar slowly decaying oscillations we find also oscillations of higher frequency which do not disappear completely. This behavior was to be expected from the stability analysis of the fixed point B^- for the complete system, where we found from Eq. (30) besides the stability exponents of the DST solution a pair $\lambda=\pm ir$ describing fast oscillations. However, the location of the fixed point and the center of the oscillations in Figs. 2, 3, and 5 are not exactly the same. The full dynamic model tends to oscillate around a state which is even more localized than predicted and consequently it decays slightly slower. Moreover, the period of the fast oscillations is of the order of $2\pi/r$ but does not quite agree with this value and is actually close to half of it. We will come back to this point when we discuss the adiabatic case in the next section.

Unlike in the figures discussed so far, a qualitative difference in the behavior of the three solutions prepared with total energy 0 is observed for $p=3$ and $g=0.1$ when they are compared to the low-energy DST and polaron (0) solutions. In Fig. 4(b) beside the latter two the bare exciton is shown for which the oscillations around the initially existing self-trapped state B^- are so large that this state is hardly recognized at all. It disappears at $\tau\sim 10$ and thus, much earlier than for the DST and polaron (0) case. The other two polaron solutions which are not displayed resemble the bare exciton. This behavior can be understood from the fact that the system with $g=0.1$ is very similar to the sinkless case which has been shown to be strongly chaotic for $r=1$ and p above the bifurcation value 1.[21] Due to the chaos, the system explores the energetically accessible phase space very fast and this is reflected in the strong and irregular oscillations of the relative site occupation leading to a rapid exciton decay. A behavior like that for the bare exciton, which compared to the low-energy DST and polaron (0) solutions is in a high-energy state, can be expected for any state prepared initially with a vibrational excess energy. In particular, an optical excitation of the dimer, which creates an electronic excitation on both sites with unrelaxed oscillator configurations, belongs to this class. For strong nonlinearity excitations of this kind are expected to leave the inital state very rapidly.

D. Time evolution in the adiabatic case

The conclusion of Sec. III B was that there is an exponential decay once the system is close to the attractive adiabatic state. However, there are two important limitations to this conclusion.

First, the initial state of the exciton has to be close to one of the adiabatic states. We consider the initially completely localized state of the exciton $\cos\theta=-1$, i.e., the initial oscillator coordinate should correspond to a strongly localized adiabatic state. According to Eq. (40) this is the case if $g^2+2pr^2Q(0)^2\gg 1$. For the bare exciton $Q(0)=0$ this is satisfied for large sink rate g and then the total occupation will decay close to the linear dimer and independent of the actual strength p of the coupling. For the polaron we have

$$g^2+2pr^2Q(0)^2=g^2+p^2\gg 1 \tag{47}$$

and the exciton can be close to an adiabatic state even for small sink rate provided the coupling to the oscillator is strong enough. The total probability decays in this case as

$$R(\tau)\sim\exp\left(-\frac{g/2}{g^2+p^2}\tau\right) \tag{48}$$

which is initially very close to what is predicted from the quasistationary decay mode B^- (34). The largest possible decay rate is according to Eq. (48) $1/4p$ and it is realized for $p=g$.

The second condition for an exponential decay of the occupation probability is that the oscillator dynamics is actually sufficiently slow to be completely disregarded during the lifetime of the exciton. According to Eq. (48) this means

$$r\ll\frac{g/2}{g^2+p^2}, \tag{49}$$

but the restriction of the exciton to one of the adiabatic states prescribed by the oscillator is justified whenever $r\ll 1$, and this can be a much weaker condition. So if in the adiabatic regime the condition (49) is not satisfied, no self-contained equation for the decay of the exciton is available.

This is the situation in Fig. 6. The parameter $r=0.1$ is sufficiently small for the application of the adiabatic approximation. Consequently, in part (b) of the figure the polaron (–) solution can be seen to follow the evolution of one of the adiabatic states, namely the energetically lower state obtained from the solution of Eq. (36). Initially, some decaying oscillations around the adiabatic state can be observed which are in good agreement with the stability exponents (37). When the adiabatic state enters the region $\cos\theta>0$ it becomes a repeller and one observes increasing oscillations around it until the variable Q has completed one full period at $\tau\sim 80$ and the relaxation to the attractor starts again.

The same behavior can be observed for the other two polaronic solutions. The excitation decays rapidly as soon as the exciton is driven by the oscillator to the sink site. Therefore in this case the lifetime of the excitation is basically determined by the frequency of the oscillator and its initial conditions. Since the polaron (–) has an initial momentum which is directed towards increasing polarization, the exciton remains for a long initial period localized on the site without sink. This period is shorter for the polaron (+) which has a

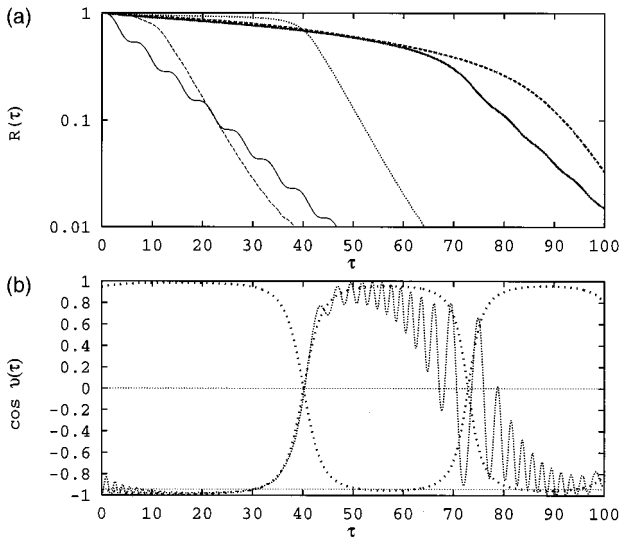

FIG. 6. Time dependence of the total occupation for all initial conditions (a) and of the relative site occupation difference for the polaron (–) (b). With the sparse bold dots the time dependence of the two adiabatic states is indicated. The parameters are $g=0.1$, $p=3$, and $r=0.1$.

momentum towards decreasing polarization and consequently the polaron (–) has a longer lifetime. The polaron (0) has no momentum at $\tau=0$ and decays initially at a rate in between the other two polarons. Due to the lacking vibrational energy the oscillator coordinate for the polaron (0) changes its position only very slowly such that the polaron (0) is the longest living solution.

Comparing in Fig. 6(a) the polaron (0) to the DST exciton we find a good agreement up to the crossover time for the DST solution. Then the DST exciton can be seen to decay faster than the polaron (0). The reason is that the initially localized state of the exciton has for the two solutions different sources. For the DST solution it results from self-trapping on the attractive fixed point B^- which keeps the exciton localized as long as it is far from its threshold of existence. Once this threshold is reached, the exciton becomes delocalized and decays rapidly. In contrast, the initial localization of the polaron (0) is *not* due to self-trapping but simply a consequence of the fact that the system was prepared in a DST state which it leaves only very slowly as it follows the oscillator position. This interpretation is further confirmed by the observation that the initial agreement between the DST and the polaron (0) solution ceases to exist as soon as the parameters do not support a self-trapped state for the DST case. The polaronic solutions are unaffected by this and still display an initial tendency towards localization on the sinkless site (not displayed). Among them the polaron (+) again decays fastest while the polaron (–) is the longest living solution.

The situation is similar in Fig. 7. The DST exciton relaxes due to the strong sink quite fast to the final location of the fixed point B^- and then decays without further oscillations, while the polaron (0), due to its inertness, remains for a longer time close to its initial position and decays consequently slower than the DST solution. All the polarons as well as the bare exciton keep oscillating around a mean value

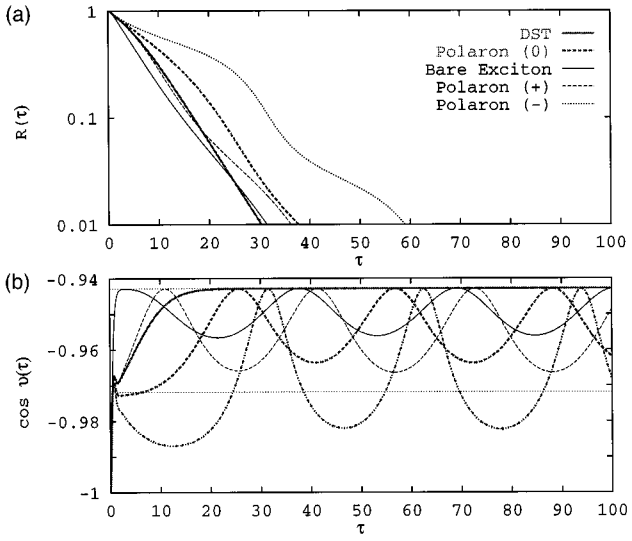

FIG. 7. Time dependence of the total occupation (a) and of the relative site occupation difference (b) for $g=3$, $p=3$, and $r=0.1$. In the bottom plot for the polaron (–) solution beside the relative site occupation the time dependence of the lower adiabatic state is displayed with sparse bold dots.

which is slightly below the location of the fixed point B^-. In fact Fig. 7(b) looks very much like the plots for $g=3$ and $p=3$ at high and intermediate frequency Fig. 3(b) and Fig. 5(b), just the deviation from the location of the point B^- is larger and the oscillations are slower. But now we can provide a more satisfactory explanation for this behavior using the adiabatic states. The polarons as well as the bare exciton follow after a very short relaxation the adiabatic state at $\cos\theta<0$. As an example for this behavior the adiabatic state for the polaron (–) is displayed in Fig. 5(b) with sparse fat dots. The location of the adiabatic state can be seen from Eq. (39) to depend on the squared amplitude of the oscillator coordinate. The localization is weakest for $Q=0$, when the adiabatic state coincides with the point B^-. The quadratic rather than linear dependence on Q is the reason why the adiabatic oscillations in the relative site occupation observed in Fig. 5(b) have a mean value below B^- and a frequency which is exactly half that of the oscillator.

In contrast to all the other solutions, the bare exciton remains completely unaffected by the nonlinearity in the adiabatic case. Here, the oscillator is prepared at $Q=0$ and there it stays during the whole lifetime of the excitation provided the adiabatic parameter r is sufficiently small. Consequently, the vibronic coupling has no effect on the exciton and it oscillates independent on p around $\cos\theta=0$ for $g<1$ (Fig. 6) or relaxes to $\cos\theta=\sqrt{1-1/g^2}$ otherwise (Fig. 8). When the coupling parameter p is small, the bare exciton is well approximated by the DST solution. In the adiabatic regime $r\ll 1$ the bare exciton shows among the different considered solutions at least initially the fastest decay.

Finally we would like to discuss an example in which the condition (49) for an exponential decay of the polaron solutions is satisfied (Fig. 8). In this case the polarons do not differ very much from each other and clearly follow an exponential law at a rate very close to that predicted by Eq. (48). Since we chose $p=g$ for the figure, the lifetime of the

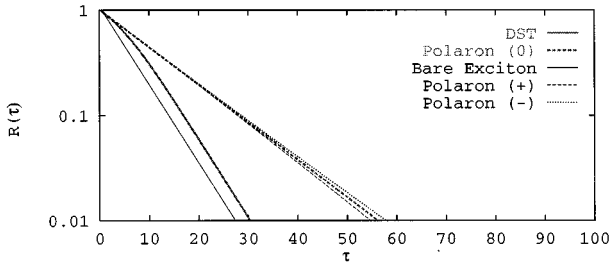

FIG. 8. Time dependence of the total occupation for $g=3$, $p=3$, and $r=0.001$.

polarons is exactly twice that of the bare exciton. The little remaining difference between the polaronic solutions reflects the residual change in the oscillator position during the lifetime of the excitation which enhances the localization of the exciton for the polaron (–) and diminishes it for the polaron (+) while there is no such effect for the polaron (0).

V. CONCLUSIONS

We have studied the decay of an exciton coupled to polarization vibrations on a dimer. Quasistationary decay modes were identified which allow us to explain the basic properties of the system. Using numerical simulations the deviations from the predicted behavior were investigated.

The model exhibits a rich variety of dynamical regimes depending on the parameters and the initial conditions. We found effects such as the time-dependent bifurcation and the associated crossover in the decay regime which are genuinely due to the interplay between the sink and the vibrational coupling and cannot be explained by considering one of these mechanisms alone.

The tendency to form an initially localized exciton state on the site without sink is enhanced by both, vibrational coupling, and trapping due to the sink. For high and intermediate oscillator frequency the system changes its behavior profoundly when the threshold for an initially self-trapped state is reached, while there is no such effect in the adiabatic regime.

The relation between the DST approximation and a mixed quantum-classical description, taking the oscillator dynamics explicitly into account, was clarified. For high oscillator frequency the influence of the oscillator initial condition is weak and the two models behave very much the same. In the adiabatic regime the bare exciton is close to the DST solution provided that the coupling is weak.

Throughout our numerical investigations the exciton was supposed to be initially localized at the site without sink. This corresponds to the experimental situation, e.g., in photosynthetic units. Of course there might exist applications of the model for which the exciton is created in a different state, but it is beyond the scope of the present paper to discuss all possible cases in detail. In general we can say that the fixed point analysis of Sec. III remains valid and can again be used to discuss the time evolution of the system. However, when doing so one must check whether the assumption of a quasistationary decay is really justified. For example in the case of a symmetric creation of the exciton over the two dimer sites and for $g^2+p^2>1$, the condition (33) is not satisfied

initially and hence the results of Sec. III A are not applicable in the most interesting initial stage of the dynamics. On the other hand, the asymptotic quasistationary decay regime for large time is independent on the initial condition and again determined by the stable fixed point B^- for $g>1$ or by $A^{\pm}$ for $g<1$. Moreover, all our results for the adiabatic regime can be easily extended to include different initial conditions of the exciton, since in this case the initial condition of the oscillator is the decisive one for the decay dynamics. We note that this latter observation means that a careful description of the exciton creation process is indispensable for a satisfactory description of the system. Finally we would like to mention that other interesting possibilities to extend the model discussed in this paper are the inclusion of dissipation and/or quantum fluctuations into the description of the oscillator.

ACKNOWLEDGMENTS

Support from the Deutsche Forschungsgemeinschaft (DFG) is gratefully acknowledged. Moreover one of us (I.B.) has enjoyed support from the project GAUK 105/95 and from the Deutscher Akademischer Austauschdienst (DAAD). While preparing this work, the authors experienced the kind hospitality of the Humboldt University, Berlin and the Charles University, Prague during mutual visits.

*Present address: Max-Planck Institut für Physik komplexer Systeme, Bayreuther Str. 40, Haus 16, 01 187 Dresden, Germany. Electronic address: holger@mpipks-dresden.mpg.de

[1] H. Haken and P. Reineker, in *Excitons, Magnons, and Phonons in Molecular Crystals*, edited by A. B. Zahlan (Cambridge University Press, Cambridge, 1968).
[2] M. Grover and R. Silbey, J. Chem. Phys. **54**, 4843 (1970).
[3] V. M. Kenkre, E. W. Montroll, and M. F. Shlesinger, J. Stat. Phys. **9**, 45 (1973).
[4] R. Kühne and P. Reineker, Z. Phys. B **22**, 201 (1975).
[5] V. M. Kenkre, in *Exciton Dynamics in Molecular Crystals and Aggregates*, Vol. 94 of *Springer Tracts in Modern Physics*, edited by G. Höhler (Springer, Berlin, 1982), pp. 1–109.
[6] P. Reineker, in *Exciton Dynamics in Molecular Crystals and Aggregates* (Ref. 5), pp. 111–226.
[7] R. M. Pearlstein and H. Zuber, in *Antennas and Reaction Centers of Photosynthetic Bacteria*, edited by M. E. Michel-Beyerle, *Springer Series in Chemical Physics*, Vol. 42 (Springer, Berlin, 1985).
[8] V. Čápek and V. Szöcs, Phys. Status Solidi B, **125**, K137 (1984).
[9] I. Barvík, in *Large Scale Molecular Systems*, Vol. 258 of *NATO Advanced Studies Institute, Series B*, Physics, edited by W. Gans, A. Blumer, and A. Aman (Plenum Press, New York, 1991), pp. 371–374.
[10] I. Barvík, in *Dynamical Processes in Condensed Molecular Systems*, edited by A. Blumen (World Scientific, Singapore, 1991), pp. 275–287.
[11] I. Barvík and P. Heřman, Phys. Status Solidi B, **174**, 99 (1991); Czech. J. Phys. **41**, 1265 (1991); Phys. Rev. B **45**, 2772 (1992).
[12] P. Heřman and I. Barvík, Phys. Lett. A **163**, 313 (1992); Phys. Rev. B **48**, 3130 (1993).
[13] P. Chvosta and I. Barvík, Z. Phys. B **85**, 227 (1991).
[14] J. Appel, Solid State Phys. **21**, 193 (1968).
[15] A. S. Davydov, *Theory of Molecular Excitons* (Plenum, New York, 1979).
[16] M. Quack, J. Mol. Struct. **292**, 171 (1993).
[17] J. C. Eilbeck, P. S. Lomdahl, and A. C. Scott, Physica D **16**, 318 (1985).
[18] V. M. Kenkre and D. K. Campbell, Phys. Rev. B **34**, 4959 (1986).
[19] B. Esser and D. Hennig, Z. Phys. B **83**, 285 (1991); Phys. Rev. A **46**, 4569 (1992).
[20] M. Kus and V. M. Kenkre, Physica D **79**, 409 (1994).
[21] B. Esser and H. Schanz, *Chaos Solitons Fractals* **4**, 2067 (1994); Z. Phys. B **96**, 553 (1995).
[22] H. Schanz and B. Esser, Z. Phys. B **101**, 299 (1996); Phys. Rev. A (to be published).
[23] V. M. Kenkre and H. L. Wu, Phys. Rev. B **39**, 6907 (1989).
[24] D. Vitali, P. Allegrini, and P. Grigolini, Chem. Phys. **180**, 297 (1994).
[25] V. Szöcs, P. Baňacký, and P. Reineker, Chem. Phys. **199**, 1 (1995).
[26] A. Osuka, K. Marnyama, and I. Yamzaki, Chem. Phys. Lett. **165**, 392 (1990).
[27] U. Rempel, B. von Maltzan, and C. von Borczyskowski, Chem. Phys. Lett. **169**, 347 (1990).
[28] R. van Grondelle *et al.*, Biochim. Biophys. Acta **1187**, 1 (1994).
[29] G. McDermott *et al.*, Nature (London) **374**, 517 (1995).
[30] I. Barvík, B. Esser, and H. Schanz, Phys. Rev. B **52**, 9377 (1995).
[31] R. Knox, Photochem. Photobiol. **57**, 40 (1993).
[32] F. Verhulst, *Nonlinear Differential Equations and Dynamical Systems* (Springer, Berlin, 1990).
[33] D. Hennig and B. Esser, Z. Phys. B **88**, 231 (1992).